Theory of Trickle-Bed Magnetohydrodynamics under Magnetic-Field Gradients

Ion Iliuta and Faïçal Larachi
Chemical Engineering Dept. and CERPIC, Laval University, Québec, G1K 7P4, Canada

External inhomogeneous magnetic fields exert a body force (magnetization force) on electrically nonconducting and magnetically permeable fluids. The force acts on both paramagnetic and diamagnetic fluids and can be used to compensate for or to amplify the gravitational body force, unlike the Lorentz braking force that manifests only for electrically conducting liquids, such as liquid metals. The ability to influence two-phase flows through porous media by the application of external inhomogeneous magnetic fields is of interest in the operation of trickle-bed reactors for catalytic process intensification, particularly in oxidation catalysis, where the O_2 paramagnetic properties may be propitious to macrogravity operation for enhancing liquid holdup and wetting efficiency. An isothermal 1-D two-fluid magnetohydrodynamics model based on volume-average mass and momentum balance equations to describe the gas-liquid downflow under a spatially uniform magnetic-field gradient. The slit model approximation was used for the derivation of drag force closures intervening in the momentum equations. The evolution of the trickle-bed magnetohydrodynamics was theoretically investigated in terms of liquid holdup and pressure drop under four gas-liquid combinations. Advantages of this novel approach of process intensification were rationalized in terms of catalytic reactions.

Introduction

The ability to influence two-phase flows by the application of external inhomogeneous magnetic fields is of potential interest in the operation of trickle-bed reactors from the point of view of process intensification for catalytic reactions. The damping of flow through application of magnetically *homogeneous* fields is applicable only to liquids exhibiting significant electrical conductivity, such as liquid metals and melts, by exploiting the Lorenz force (Branover, 1978; Iliuta and Larachi, 2003). Obviously, this prospect has poor potential applicability in multiphase catalytic reactor engineering because most of the process fluids, water-like or organic as well as the gases, are either electrically nonconducting or weakly conducting. The force exploited in the present investigation has a different origin and is independent of the fluid electrical conductivity. The magnetization force, *per se*, is a body force that is analogous to the gravitational force and manifests when *inhomogeneous* magnetic fields are applied to paramagnetic or diamagnetic materials in phase α (gas, liquid, solids)

$$F_{M\alpha} = \frac{\chi_\alpha}{\mu_0} B \frac{dB}{dz} = \mu_0 \chi_\alpha H \frac{dH}{dz} \tag{1}$$

where the volume susceptibility χ_α is similar to the density, and the one-dimensional (1-D) magnetic field gradient BdB/dz exerts a body force similar to the gravitational force.

In general, the magnetization force in a paramagnetic fluid ($\chi_\alpha > 0$) is much larger than in a diamagnetic fluid ($\chi_\alpha < 0$). The paramagnetic fluids contain atoms or molecules that possess an intrinsic magnetic moment, and their magnetic susceptibilities satisfy Curie's law. Unlike paramagnetic fluids, diamagnetic fluids contain atoms or molecules that do not exhibit intrinsic magnetic moment. When a *static* magnetic field is applied to these fluids, the change of the field induces a magnetic moment for each atom or molecules. The diamagnetic fluids experience a weak *repulsive* force in an inhomogeneous magnetic field, while the paramagnetic fluids experience a much larger *attractive* force.

Correspondence concerning this article should be addressed to F. Larachi.

Compared with gravitational force, it is a remarkable characteristic that the direction of the magnetization force can be controlled so that sub- or macrogravity conditions can be artificially realized in either or both gas and liquid in the two-phase flow prevailing in trickle-bed reactors.

The method of controlling vertical acceleration has found many applications over a wide range of fundamental research such as in the formation of high-quality crystals, the synthesis of new materials, and also in fluid dynamics experiments (Wakayama et al., 2001). Recently, there have been some reports that an upward magnetization force reduces the effect of gravity. For example, Beaugnon and Tournier (1991) and Ikezoe et al. (1998) succeeded in levitating water, ethanol, and acetone by applying an inhomogeneous magnetic field and producing an upward magnetization force. Magnetic levitation occurs when the integrated upward magnetization force is *counterbalanced* by the gravitational force. Furthermore, it was found that the vertical magnetization force has an influence on the process of protein crystal formation (Wakayama et al., 1997). When either an upward or a downward magnetization force was applied to supersaturated protein solutions, the quality of protein crystals was found to improve or deteriorate, respectively (Lin et al., 2000). Magnetic buoyancy force was observed experimentally to affect the motion of bubbles in their way in paramagnetic and diamagnetic liquids (Wakayama, 1997; Wakayama et al., 2001). When an upward magnetization force acts on the fluid, vertical acceleration (effective gravity) can be reduced from 1 unit g to almost 0 g (Wakayama et al., 1997, 2001) entraining damping of natural convection and its adverse effects (Wang and Wakayama, 2002). The influence of inhomogeneous magnetic fields on natural convection was also studied theoretically. Qi and Wakayama (2000), Qi et al. (2001), and Ramachandran and Leslie (2001) studied numerically the natural convection of the Rayleigh-Benard type in cylindrical enclosures with vertically oriented magnetization force. Very recently, Wang and Wakayama (2002) published a detailed numerical study on the ways of controlling natural convection in non- and low-conducting diamagnetic fluids contained in cubical enclosures under inhomogeneous magnetic fields oriented in different directions.

In contrast, information about analogous magnetohydrodynamic phenomena taking place in trickle-bed reactors under inhomogeneous magnetic fields, and involving the flow of nonconducting, magnetically permeable fluids, is still largely *terra incognita*. The ability to influence two-phase flows through porous media by the application of external inhomogeneous magnetic fields may be of major interest in the oper-

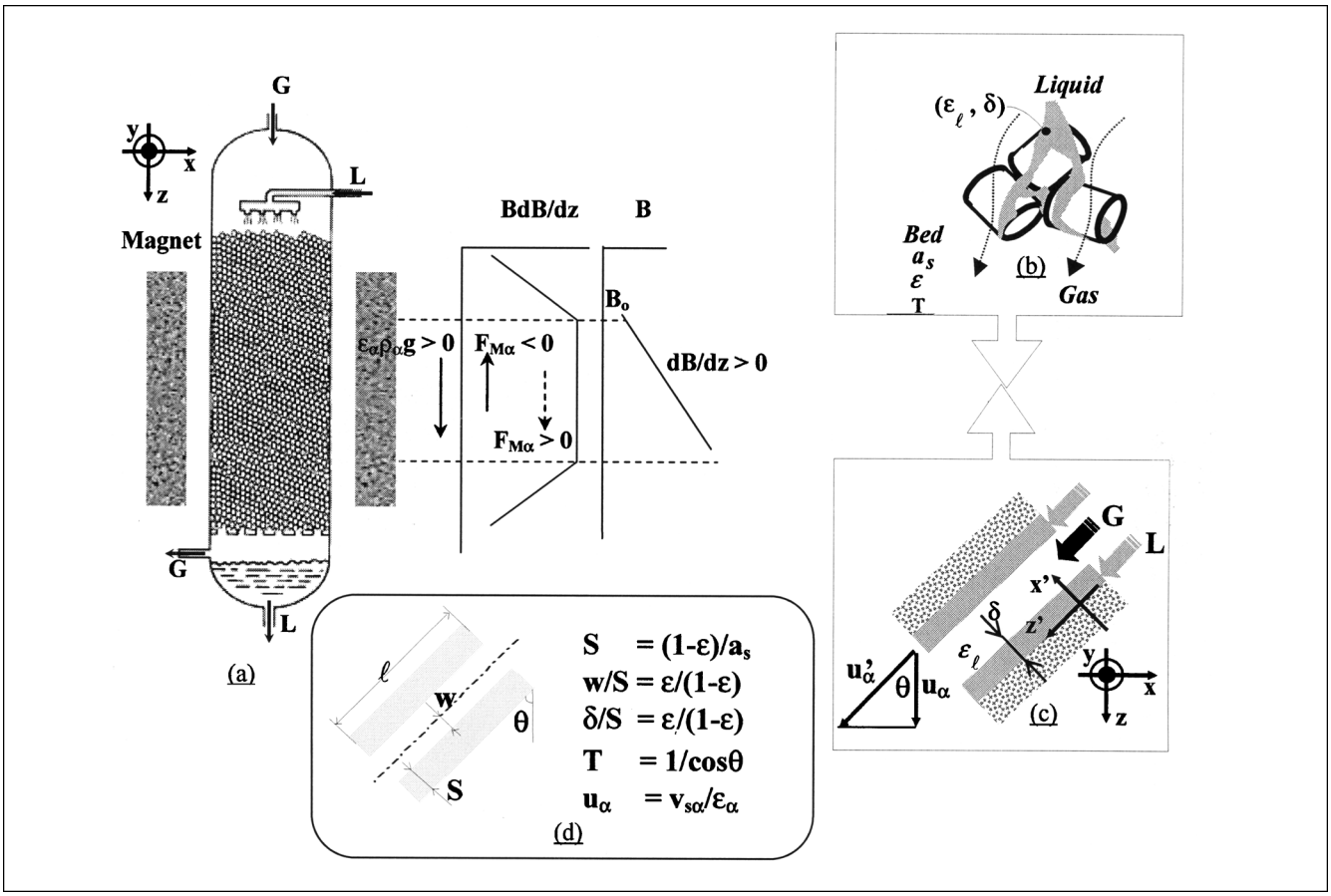

Figure 1. (a) Relationship between magnetization and gravitational forces acting on fluid flow in a trickle bed reactor (with the magnitude of BdB/dz spatially uniform); (b) actual gas-liquid flow pattern in trickle flow regime, (c) conceptual slit flow; (d) slit geometry.

ation of trickle-bed reactors, especially in mini- or microsized reactors, from the standpoint of catalytic process intensification. In particular for reactors hosting catalyst-mediated oxidation in organic liquids, the paramagnetic properties of O_2 present in the gas phase combined with the diamagnetic organic liquid properties, may represent a propitious factor to generate macrogravity operation for improving liquid holdup and wetting efficiency and for reducing hydraulic energy consumption or pressure drop.

To explore numerically the impact of a spatially *uniform* magnetic-field gradient in a trickle-bed reactor, an isothermal 1-D two-fluid magnetohydrodynamics model based on the volume-average mass and momentum balance equations was developed to describe the gas-liquid downflow in terms of liquid holdup and pressure drop predictions under four gas-liquid combinations: paramagnetic gas–diamagnetic liquid, paramagnetic gas–paramagnetic liquid, and diamagnetic gas–diamagnetic liquid, and diamagnetic gas–paramagnetic liquid.

Governing Equations of Trickle-Flow Magnetohydrodynamics

Volume-average balance equations

A two-phase downward gas-liquid trickle flow through a porous medium in the presence of spatially uniform magnetic field gradient was considered (Figure 1a). The direction of the magnetic field is parallel to the column axis and the gravity. The two-phase flow was assumed unidirectional, without chemical reaction, with both flowing phases viscous Newtonian. The liquid was incompressible and the gas phase ideal. The packing surface was totally wet by a film-like liquid flow, while the gas flows amid solid and liquid in the remaining interstitial space (Figure 1b).

Figure 1a illustrates both upwardly and downwardly oriented magnetization forces ($F_{M\alpha}$) acting on phase α to promote, correspondingly, subgravity or macrogravity conditions. For illustration purposes in Figure 1a, the magnetic-field gradient dB/*dz* was arbitrarily chosen so as to produce a magnetic field linearly *increasing* in the streamwise direction (that is, downwards). In practice, negative and positive magnetic-field gradients can be produced alike depending on the relative position in the magnet bore of the reactor with respect to the central point where B is maximum. In the particular configuration of Figure 1a, paramagnetic fluids ($\chi_\alpha > 0$) undergo positive magnetization force which adds up with the gravitational force to create macrogravity conditions in the fluid. Conversely, diamagnetic fluids ($\chi_\alpha < 0$) give rise to a negative magnetization force lowering the impact of gravitation.

Furthermore, each fluid phase is viewed as a continuum for which the differential-macroscopic balance equations can be applied. The model was based on the volume-average form of the transport equations for multiphase systems (Whitaker, 1973). The model equations consist of the conservation of volume, conservation of mass, and conservation of momentum for the gas and liquid phases:

Conservation of volume

$$\epsilon_\ell + \epsilon_g = \epsilon \tag{2}$$

Continuity for the gas and liquid phases.

$$\frac{\partial}{\partial t}(\epsilon_g \rho_g) + \frac{\partial}{\partial z}(\epsilon_g \rho_g u_g) = 0 \tag{3}$$

$$\frac{\partial}{\partial t}(\epsilon_\ell \rho_\ell) + \frac{\partial}{\partial z}(\epsilon_\ell \rho_\ell u_\ell) = 0 \tag{4}$$

Momentum balance equations for the gas and liquid phases.

$$\frac{\partial}{\partial t}(\rho_g \epsilon_g u_g) + u_g \frac{\partial}{\partial z}(\rho_g \epsilon_g u_g) = \epsilon_g \mu_g^e \frac{\partial^2 u_g}{\partial z^2} - \epsilon_g \frac{\partial P_g}{\partial z} + \epsilon_g \rho_g g - F_{g\ell} + F_{Mg}\epsilon_g \tag{5}$$

$$\frac{\partial}{\partial t}(\rho_\ell \epsilon_\ell u_\ell) + u_\ell \frac{\partial}{\partial z}(\rho_\ell \epsilon_\ell u_\ell) = \epsilon_\ell u_\ell^e \frac{\partial^2 u_\ell}{\partial z^2} - \epsilon_\ell \frac{\partial P_\ell}{\partial z} + \epsilon_\ell \rho_\ell g + F_{g\ell} - F_{\ell s} + F_{M\ell}\epsilon_\ell \tag{6}$$

To close the system made up of Eqs. 2–6, specification of closures for the volume-average interfacial drag forces and for magnetization forces are needed.

Drag force closure expressions

In the momentum balance Eqs. 5 and 6, a set of constitutive equations is required for the interfacial drag forces. The assumption of bed complete wetting entrains that the gas-phase drag will only have contributions due to effects located at the gas-liquid interface. The resultant of these forces denoted $F_{g\ell}$ is the drag force exerted on the gas phase as a result of the relative motion between the flowing phases to oppose slip. Similarly, the resultant of the forces exerted on the liquid phase involves two components: (a) the drag force $F_{\ell s}$, experienced by the liquid due to the shear stress nearby the liquid-solid boundary; (b) and the gas-liquid interfacial drag $F_{g\ell}$.

Under the circumstances of trickle-flow regime, the slit flow analogy can give a satisfactory approximation of the constitutive equations needed for the gas-liquid and the liquid-solid drag forces (Holub et al., 1992; Iliuta et al., 2000). The gas-liquid (inclined) slit flow, illustrated in Figure 1c, becomes well representative of this gas-continuous flow regime when the liquid texture is mainly contributed by the packing-supported liquid films and rivulets, so that the gas-liquid separated flow assumption holds. This is generally true at low liquid flow rates that allow the transport of liquid in the form of a smooth and stable film (Holub et al., 1992). The geometric mapping relations between the bed and slit scales are shown in Figure 1d.

The actual trickle-flow structure being conceptualized via an idealized slit flow, the force balance equations for the gas and liquid are first solved in the slit scale and then mapped into the bed scale. Iliuta et al. (2002) identified the liquid-solid and the gas-liquid drag forces based on the slit analogy. Under the conditions of enhanced gas-liquid interfacial interac-

tions, the projections of the drag forces at a given depth z in the bed take the following forms

$$F_{\ell s} = \left\{ E_1 \frac{(1-\epsilon)^2 \mu_\ell}{d_p^2 \epsilon_\ell^3} + E_2(1+\psi_{g\ell}) \frac{1-\epsilon}{d_p \epsilon_\ell^3} \rho_\ell \mid v_{S\ell} \mid \right\} v_{S\ell} \epsilon_\ell \tag{7}$$

$$F_{g\ell} = \left\{ E_\ell \frac{(1-\epsilon)^2 \mu_g}{d_p^2 \epsilon_g^3} + E_2(1+\psi_{g\ell}) \frac{(1-\epsilon)\rho_g}{d_p \epsilon_g^3} \mid v_{Sg} - \epsilon_g u_{g,i} \mid \right\} \times (v_{Sg} - \epsilon_g u_{g,i}) \epsilon_g \tag{8}$$

Formulation of liquid (or gas) interfacial velocity under magnetic-field gradient

Velocity continuity condition at the gas-liquid interface entails that the gas and the liquid velocities are equal there. The liquid interfacial velocity was obtained by solving the 1-D projection of the momentum balance equation along direction x' for a Newtonian incompressible liquid moving in the gravitational direction with a magnetic field gradient superimposed in the z direction (Figure 1c)

$$-\mu_\ell \frac{d^2 u'_\ell}{dx'^2} = \left(\rho_\ell g - \frac{dP}{dz} \right) \cos\theta + F_{M\ell} \cos\theta \tag{9}$$

with the boundary conditions

$$x' = 0 \qquad u'_\ell = u'_{\ell,i} = u'_{g,i} \tag{10}$$

$$\mu_g \frac{\partial u'_g}{\partial x'} = \mu_\ell \frac{\partial u'_\ell}{\partial x'} \tag{11}$$

$$x' = \delta \qquad u'_\ell = 0 \tag{12}$$

Double integration of Eq. 9 (using the boundary conditions Eqs. 10 and 12) yields the velocity distribution of the liquid in the slit

$$u'_\ell(x') = -\frac{1}{\mu_\ell} \left(\rho_\ell g - \frac{dP}{dz} + F_{M\ell} \right) \frac{x'^2}{2} \cos\theta + \frac{1}{\mu_\ell} \left(\rho_\ell g - \frac{dP}{dz} + F_{M\ell} \right) \frac{x'}{2} \delta \cos\theta + u'_{\ell,i} \left(1 - \frac{x'}{\delta} \right) \tag{13}$$

A force balance over the control volume delineated by the gas domain in the wet slit gives

$$\left(-\frac{dP}{dz} + \rho_g g + F_{Mg} \right) \cos\theta = \frac{\eta_e \tau_{ig}}{(w-\delta)\eta_e} \tag{14}$$

The interfacial shear stress obtained from the derivative of Eq. 13 at $x = 0$ is equated to that given by Eq. 14, through application of boundary condition Eq. 11, to finally obtain the following expression for the interfacial velocity in the slit scale

$$u'_{\ell,i} = \frac{\delta^2}{2\mu_\ell} \left(-\frac{dP}{dz} + \rho_\ell g + F_{M\ell} \right) \cos\theta + \frac{\delta(w-\delta)}{\mu_\ell} \left(-\frac{dP}{dz} + \rho_g g + F_{Mg} \right) \cos\theta \tag{15}$$

After further transformation using the relations shown in Figure 1d, the resulting equation for the liquid interfacial velocity in the bed scale becomes

$$u_{\ell,i} = \frac{36}{E_1 \mu_\ell} \left(-\frac{dP}{dz} + \rho_\ell g + F_{M\ell} \right) \left(\frac{\epsilon_\ell}{a_s} \right)^2 + \frac{72}{E_1 \mu_\ell} \left(-\frac{dP}{dz} + \rho_g g + F_{Mg} \right) \frac{\epsilon_\ell (\epsilon - \epsilon_\ell)}{a_s^2} \tag{16}$$

Two-phase flow stationary model

Assuming that liquid holdup does not vary appreciably along the vertical direction enables the neglect of capillary pressure gradient with respect to the fluid pressure gradient (Attou et al., 1999)

$$\frac{dP_g}{dz} = \frac{dP_\ell}{dz} = \frac{dP}{dz} \tag{17}$$

Assuming further that a steady-state flow prevails, the differential-macroscopic balance equations for the gas and liquid phases can be rewritten as follows

$$\epsilon_\ell + \epsilon_g = \epsilon \tag{18}$$

$$\frac{1}{u_g} \frac{du_g}{dz} + \frac{1}{\epsilon_g} \frac{d\epsilon_g}{dz} + \frac{1}{P} \frac{dP}{dz} = 0 \tag{19}$$

$$\frac{1}{u_\ell} \frac{du_\ell}{dz} + \frac{1}{\epsilon_\ell} \frac{d\epsilon_\ell}{dz} = 0 \tag{20}$$

$$\epsilon_g \rho_g u_g \frac{du_g}{dz} = \epsilon_g \mu_g^e \frac{d^2 u_g}{dz^2} - \epsilon_g \frac{dP}{dz} + \epsilon_g \rho_g g - F_{g\ell} + F_{Mg} \epsilon_g \tag{21}$$

$$\epsilon_\ell \rho_\ell \mu_\ell \frac{du_\ell}{dz} = \epsilon_\ell u_\ell^e \frac{d^2 u_\ell}{dz^2} - \epsilon_\ell \frac{dP}{dz} + \epsilon_\ell \rho_\ell g - F_{\ell S} + F_{g\ell} + F_{M\ell} \epsilon_\ell \tag{22}$$

Equations 18–22 establish the two-phase flow model in the form of a set of five coupled differential equations and five unknowns, that is, ϵ_g, ϵ_ℓ, u_g, u_ℓ, and P. The input variables to be fed to this model are the fluid superficial velocities, the fluid physical properties, the bed and packing characteristics, the magnetic field gradient (BdB/dz), and the interfacial velocity estimated by means of Eq. 16. The spatial discretization was performed using the standard centered finite difference scheme (a spaced mesh with 20 points was used). The

resulting nonlinear model was solved using an iterative Newton-Raphson algorithm.

Boundary conditions

At the top of the reactor, the "inlet" boundary is specified. At this boundary, the appropriate values for gas and liquid velocities are specified based on the known volume flow rates of both phases. The liquid holdup at the reactor inlet was calculated assuming $du_g/dz = du_\ell/dz = 0$ and combining Eqs. 21 and 22

$$\frac{F_{g\ell}}{\epsilon_g} + \frac{-F_{\ell s} + F_{g\ell}}{\epsilon_\ell} + (\rho_\ell - \rho_g)g - F_{Mg} + F_{M\ell} = 0 \quad (23)$$

At the bottom of the column, the "mass-flow boundary" is specified to ensure the global mass conservation.

Results and Discussion

The two-phase flow model developed earlier is free from adjustable arbitrary parameters. It can, therefore, be very helpful in exploring the impact of the most important operating variables on the two-phase pressure drop and the liquid holdup. Simulations were hence undertaken to verify whether the magnetic field gradient, the gas density, the gas and liquid velocities, and the magnetic susceptibility of the gas-liquid system are likely to bring about variations expected from knowledge of the porous medium behavior hosting the flow of nonconducting gases and liquids in the presence of an external inhomogeneous spatially uniform magnetic field gradient. The following four gas–liquid combinations were explored: paramagnetic gas–diamagnetic liquid, paramagnetic gas and liquid, diamagnetic gas and liquid, diamagnetic gas–paramagnetic liquid. Diamagnetic gas and liquid systems are typically representative for hydrogenation reactions whereas paramagnetic gas–diamagnetic liquid systems are rather representative for oxidation reactions. It is noteworthy that paramagnetic liquids are less common than diamagnetic ones. However, homogeneously catalyzed reactions within gas-liquid systems are examples where paramagnetic liquids could be encountered. In the following, we will focus on the behavior of paramagnetic gas and diamagnetic liquid systems under external inhomogeneous magnetic fields. The three other combinations involving paramagnetic gas and liquid, diamagnetic gas and liquid, and diamagnetic gas–paramagnetic liquid are approached only briefly within the heading "rationalization of the simulations."

It may be instructive to assess the relative importance of gravity vs. magnetization for each of the liquid and gas. One simple measure could be a gravitational amplification factor for the phase α (being liquid or gas), defined as

$$\gamma_\alpha = \frac{\rho_\alpha g + F_{M\alpha}}{\rho_\alpha g} \quad (24)$$

In general, three cases may arise as follows for phase α: (a) $\gamma_\alpha > 1$ macrogravity; (b) $1 > \gamma_\alpha > 0$ subgravity; (c) $\gamma_\alpha < 0$ where the weight is counter-balanced by a larger magnetization upward force.

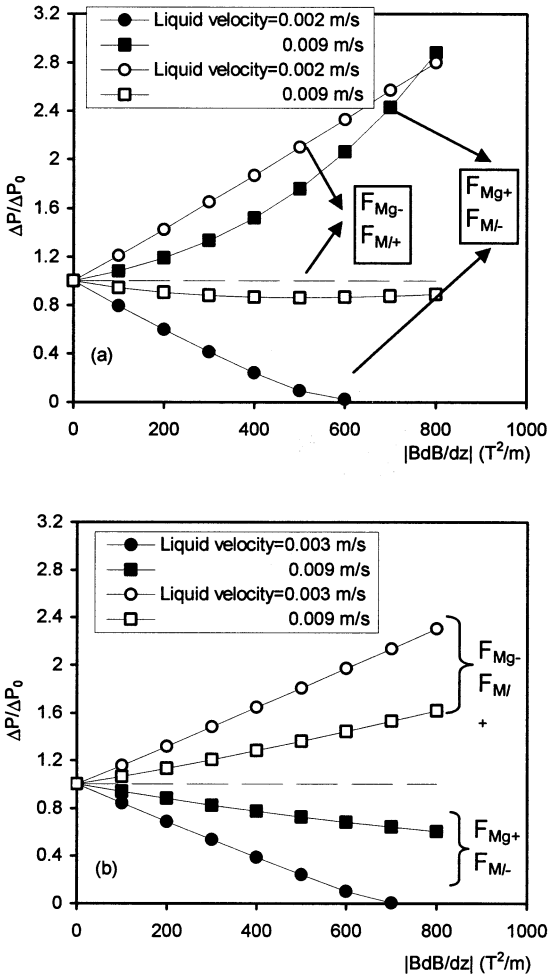

Figure 2. Effect of the external magnetic field along *z*-direction on two-phase pressure drop ratio at different liquid velocities.

Air-water system; $v_{Sg} = 0.05$m/s; $d_c = 0.051$ m; $d_p = 0.003$ m; $\epsilon = 0.37$; $E_1 = 195$; $E_2 = 1.75$; $\chi_\ell = -9.0 \times 10^{-6}$: (a) $\rho_g = 1.2$ kg/m^3 ($\chi_g = 0.379 \times 10^{-6}$); (b) $\rho_g = 60$ kg/m^3 ($\chi_g = 18.8 \times 10^{-6}$). Bed simulated length = 0.1 m.

Paramagnetic gas – diamagnetic liquid systems

When BdB/dz is negative, the magnetization force acts on the liquid phase downwardly ($\chi_\ell < 0$, macrogravity: $F_{M\ell+}$) and on the gas phase upwardly ($\chi_g > 0$, $\gamma_g < 1$: F_{Mg-}). Conversely, when BdB/dz is positive, the magnetization force acts on the liquid phase upwardly (microgravity: $F_{M\ell-}$) and on the gas phase downwardly (macrogravity: F_{Mg+}). In the case simulated here, the liquid gravitational amplification factor γ_ℓ varied in the range [1.6 : 0.4] corresponding, respectively, to BdB/dz in the range $[-800 : 800]$ T^2/m. Correspondingly, the gas gravitational amplification factor γ_g continuously evolved from -19 to $+21$.

Figures 2a and b show the effect of the external magnetic field on the total two-phase pressure drop ratio for two gas densities (atmospheric flow and high-pressure flow) and different superficial liquid velocities. The base pressure drop ΔP_0 is calculated in the case of no magnetic field (B and $dB/dz = 0$). At high pressure (Figure 2b), the gas magnetiza-

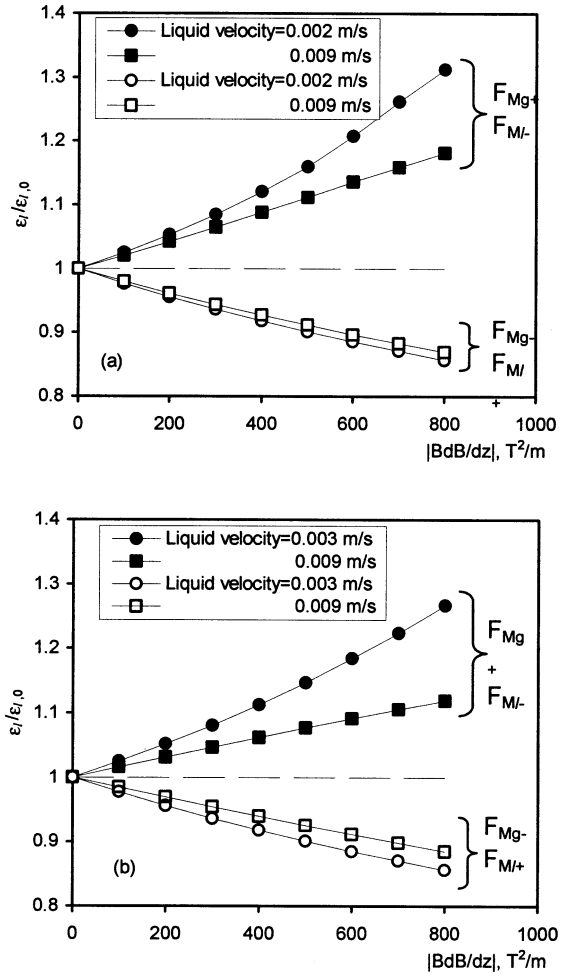

Figure 3. Effect of the external magnetic field along *z*-direction on liquid holdup ratio at different liquid velocities.

Air-water system; $v_{Sg} = 0.05$ m/s; $d_c = 0.051$ m; $d_p = 0.003$ m; $\epsilon = 0.37$; $E_1 = 195$; $E_2 = 1.75$; $\chi_\ell = -9.0 \times 10^{-6}$: (a) $\rho_g = 1.2$ kg/m^3 ($\chi_g = 0.379 \times 10^{-6}$); (b) $\rho_g = 60$ kg/m^3 ($\chi_g = 18.8 \times 10^{-6}$). Bed simulated length = 0.1 m.

tion is controlling ($|\chi_g| \gg |\chi_\ell|$) and the two-phase pressure drop can be modulated at will by applying a magnetic field gradient. For positive magnetic gradients, the downward gas magnetization force amplifies the effect of gravity (macrogravity) and two-phase pressure drop is reduced. For negative magnetic gradients, the upward gas magnetization force reduces the effect of gravity (such as sub-gravity) and two-phase pressure drop increases. This influence is very important at lower liquid velocities when the gas holdup is higher. This feature is relatively different at low pressure (Figure 2a). At high liquid velocities, the gas magnetization force is damped by the liquid magnetization force when the magnetic gradients are negative, whereas the liquid magnetization force becomes controlling when the magnetic gradients are positive. At low liquid velocities, gas magnetization is controlling.

Figures 3a and 3b depict the effect of the external magnetic field in the same simulation conditions as in Figure 2, in terms of total liquid holdup ratio at different liquid velocities and gas densities. Here, also, ϵ_{lo} is calculated in the case of no magnetic field (B and $dB/dz = 0$). Liquid holdup is a result of a balance between the two-phase pressure drop (driving force) and the resistance forces. For both low and high gas densities, when magnetic gradients are negative, liquid holdup decreases with increasing $|BdB/dz|$ because the driving force (two-phase pressure drop) increases (Figure 2). On the contrary, when the magnetic gradients are positive, the liquid holdup increases with increasing $|BdB/dz|$ because of the decrease in the driving force. On the other hand, when the magnetic gradients are positive and liquid magnetization force is controlling (low pressure), the liquid holdup increases with increasing $|BdB/dz|$ despite an increase of the two-phase pressure drop ratio. This is because the resistance to the liquid flow increases strongly with increasing $|BdB/dz|$ due to liquid magnetization force.

Figures 4a and 4b reflect the effects of the external magnetic field on the ratios of two-phase pressure drop and liquid holdup under various superficial gas velocities. At low gas velocities, the downward gas magnetization force (positive magnetic gradients) is very important and the two-phase pressure drop is reduced significantly. On the other hand, the negative magnetic field gradients promote an increase in two-phase pressure drop. At low gas velocities, the liquid holdup increases (positive gradient)/decreases (negative gradient) markedly with increasing the magnetic field gradient.

Rationalization of the simulations

Table 1 summarizes the rationalization of the simulations for the aforementioned gas-liquid combinations. It shows that an increase of BdB/dz amplifies the effect of gravity thus reducing pressure drop (exception diamagnetic gas and liquid systems). For negative BdB/dz, the upward liquid or gas magnetization forces induce subgravity conditions and an augmentation of two-phase pressure drop (exception diamagnetic gas and liquid systems).

For *paramagnetic gas and liquid systems*, liquid and gas magnetization forces are comparable ($|\chi_\ell| \approx |\chi_g|$) at high pressure. For positive magnetic gradients, the downward gas and liquid magnetization forces promote the damping of shear stresses at the liquid-solid and gas-liquid interfaces, and two-phase pressure drop is reduced significantly even at low magnetic field gradients. For negative magnetic gradients, the upward gas and liquid magnetization forces reduce the effect of gravity so that the two-phase pressure drop increases significantly. These tendencies are similar at low pressure when liquid magnetization is controlling ($|\chi_\ell| \gg |\chi_g|$) . At low pressure, the liquid holdup increases/decreases markedly with increasing $|BdB/dz|$. The liquid holdup as a function of $|BdB/dz|$ decreases (respectively, increases) with increasing positive (respectively, negative) magnetic field gradients. The variation is very marginal at high pressure.

Usually, for *diamagnetic gas-paramagnetic liquid systems*, the liquid magnetization is the controlling factor ($|\chi_\ell| \gg |\chi_g|$). For positive BdB/dz, the downward liquid magnetization force amplifies the effect of gravity thus reducing pressure drop. For negative BdB/dz, the upward liquid magnetization force induces subgravity ($0 < \gamma_\ell < 1$) or net upward body force ($\gamma_\ell < 0$) conditions, and an increase of two-phase pressure drop. This augmentation is remarkable at lower gas densities. At low pressure, liquid holdup increases/decreases markedly

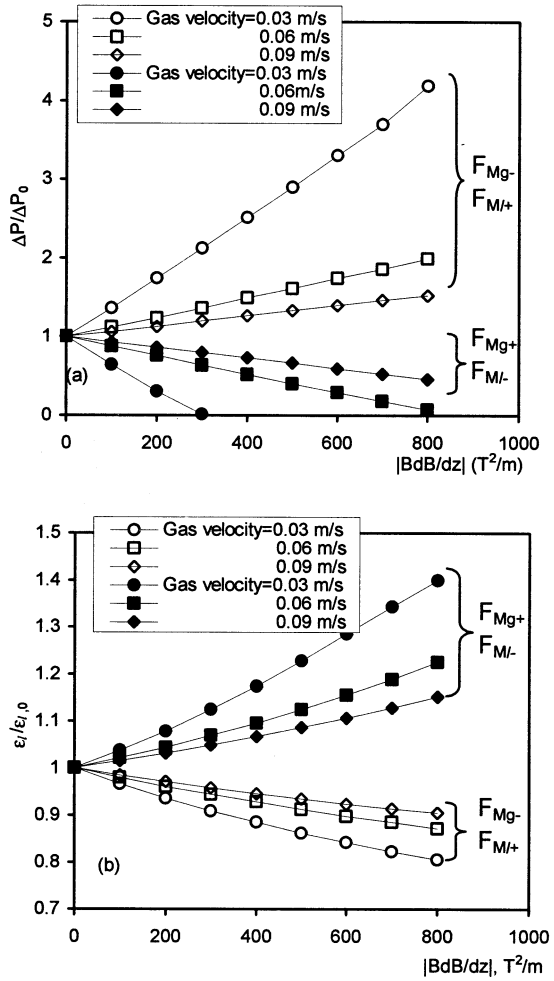

Figure 4. Effect of the external magnetic field along *z*-direction on two-phase pressure drop ratio (a) and total liquid holdup ratio (b) at different gas velocities.

Air-water system; $v_{S\ell} = 0.003$ m/s; $\rho_g = 60$ kg/m^3; $d_c = 0.051$ m; $d_p = 0.003$ m; $\epsilon = 0.37$; $E_1 = 195$; $E_2 = 1.75$; $\chi_\ell = -9.0 \times 10^{-6}$; $\chi_g = 18.8 \times 10^{-6}$). Bed simulated length = 0.1m.

with increasing $|BdB/dz|$ and the variation is very marginal at high pressure due to the prevailing lower liquid holdups.

For *diamagnetic gas and liquid systems*, the liquid magnetization is controlling ($|\chi_\ell| \gg |\chi_g|$) regardless of pressure. Negative BdB/dz yields a downward liquid magnetization force that amplifies the effect of gravity and two-phase pressure drop is reduced. For positive magnetic gradient, the upward liquid magnetization force reduces the effect of gravity and two-phase pressure drop increases. This latter influence is more important at higher liquid velocities when the liquid holdup is higher. It is worth noting that the increase (or decrease) of two-phase pressure drop with increasing magnetic field gradient is less important than in the case of paramagnetic gas/liquid systems because the volume magnetic susceptibility of diamagnetic gases and liquids is very low. Liquid holdup increases/decreases with increasing $|BdB/dz|$ and the variation is very marginal at high pressure.

Paramagnetic gas–diamagnetic liquid systems deserve particular attention. Elevated levels of magnetic field gradient improve the liquid holdup and, thus, the wetting efficiency of the catalyst particle. For liquid-reactant limited reactions (such as in oxidation reactions), both improvements contribute to increase the chemical conversion of the catalytic reaction, while, simultaneously, the two-phase pressure drop is considerably reduced.

Conclusion

The ability to influence two-phase flow by the application of an external inhomogeneous magnetic field is of potential interest in the operation of trickle-bed reactors from the point of view of catalytic process intensification. A two-fluid model based on the volume-average mass and momentum balance equations was developed for the prediction of two-phase pressure drop and liquid holdup in fixed beds operating in the trickle flow regime under the influence of an inhomogeneous magnetic field. The slit model approximation was used for the derivation of drag force closures needed in the momentum conservation equations. Simulations were undertaken to study the influence of the spatially uniform magnetic field gradient on the two-phase pressure drop and liquid holdup at different gas densities, gas and liquid velocities, and for different gas-liquid systems. The liquid and gas magnetization forces induce subgravity ($0 < \gamma_\alpha < 1$), macrogravity ($\gamma_\alpha > 1$), countergravity ($\gamma_\alpha < 0$) conditions, and a major augmentation or reduction of two-phase pressure drop. Elevated levels of magnetic field gradient improve or deteriorate appreciably the liquid holdup, and, thus, the wetting efficiency of the catalyst particle.

Notation

a_s = external area of the bed, $a_s = 6(1-\epsilon)/d_p$, m^2/m^3
B = magnetic flux density, T (Vs/m^2)

Table 1. Rationalization of the Simulations for Potential Process Intensification Routes

	Paramagnetic Gas–Diamagnetic Liquid		Paramagnetic Gas and Liquid		Diamagnetic Gas–Paramagnetic Liquid		Diamagnetic Gas & Liquid	
	$\Delta P/\Delta P0_0^*$	$\epsilon_\ell/\epsilon_{\ell,0}$	$\Delta P/\Delta P_0$	$\epsilon_\ell/\epsilon_{\ell,0}$	$\Delta P/\Delta P_0$	$\epsilon_\ell/\epsilon_{\ell,0}$	$\Delta P/\Delta P_0$	$\epsilon_\ell/\epsilon_{\ell,0}$
(BdB/$dz > 0$) ↗	↘	↗	↘	↘	↘	↘	↗	↗
(BdB/$dz < 0$) ↘	↗	↘	↗	↗‡	↗	↗	↘	↘
	F_{Mg} is controlling†		high pressure: $F_{M\ell} \approx F_{Mg}$ low pressure: $F_{M\ell} > F_{Mg}$		$F_{M\ell}$ is controlling		$F_{M\ell}$ is controlling	

*Except at low pressure and high liquid velocities.
†Except at high liquid velocities and positive magnetic gradients at low pressure.
‡Except high pressure when liquid holdup increases/decreases weakly with increasing |BdB/dz|.

d_c = column diameter, m
d_p = effective particle diameter, m
E_1, E_2 = Ergun constants
$F_{g\ell}$ = gas-liquid drag force, N/m^3
$F_{\ell s}$ = liquid-solid drag force, N/m^3
$F_{M\alpha}$ = magnetization force in α-phase, N/m^3
g = gravity acceleration, m/s^2
H = magnetic-field strength, A/m
P = pressure, Pa
R = constant of ideal gas, J/kg K
S = slit half-wall thickness, m
T = bed tortuosity, $T = 1/\cos\ \theta$
u_α = average interstitial velocity of α-fluid, m/s
u'_α = velocity of α-fluid in the slit, $\langle u'_\alpha \rangle \cos\ \theta = u_\alpha$, m/s
$u_{\alpha,i}$ = α-phase interfacial velocity, m/s
$u'_{\alpha,i}$ = α-phase interfacial velocity in the slit, $u'_{\alpha,i} \cos\ \theta = u_{\alpha,i}$, m/s
$v_{S\alpha}$ = α phase superficial velocity, m/s
w = slit half-void thickness, m

Greek letters

χ_α = volume magnetic susceptibility, dimensionless
δ = liquid film thickness, m
ϵ = bed void fraction
ϵ_α = α phase holdup
γ_α = α phase gravitational amplification factor
μ_0 = absolute magnetic permeability of vacuum, H/m
μ_α = α phase dynamic viscosity, kg/m·s
μ^e_α = α phase effective viscosity (combination of bulk and shear terms), kg/m·s
θ = slit inclination, $\cos\ \theta = \sqrt{72/E_1}$
ρ_α = density of α phase, kg/m^3
σ = surface tension, N/m
$\tau_{i\alpha}$ = α-phase interfacial shear stress, Pa
$\psi_{g\ell}$ = gas-liquid interaction parameter

Subscripts

g = gas phase
i = gas-liquid interface
ℓ = liquid phase
s = solid phase

Literature Cited

Attou, A., C. Boyer, and G. Ferschneider, "Modelling of the Hydrodynamics of the Cocurrent Gas-Liquid Trickle Flow through a Trickle-Bed Reactor," *Chem. Eng. Sci.*, **54**, 785 (1999).

Beaugnon, E., and R. Tournier, "Levitation of Organic Materials," *Nature*, **349**, 470 (1991).

Branover, H., *Magnetohydrodynamic Flows in Ducts*, Wiley, New York (1978).

Holub, R. A., M. P. Dudukovic, and P. A. Ramachandran, "A Phenomenological Model for Pressure Drop, Liquid Holdup and Flow Regimes Transition in Gas-Liquid Trickle Flow," *Chem. Eng. Sci.*, **47**, 2343 (1992).

Ikezoe, Y., N. Hirota, J. Nakagawa, and K. Kitazawa, "Making Water Levitate," *Nature*, **393**, 749 (1998).

Iliuta, I., F. Larachi, and M. H. Al-Dahhan, "Double-Slit Model for Partially Wetted Trickle Flow Hydrodynamics," *AIChE J.*, **46**, 597 (2000).

Iliuta, I., B. P. A. Grandjean, and F. Larachi, "New Mechanistic Film Model for Pressure Drop and Liquid Holdup in Trickle Flow Reactors," *Chem. Eng. Sci.*, **57**, 3359 (2002).

Iliuta, I., and F. Larachi, "Magnetohydrodynamics of Trickle Bed Reactors: Mechanistic Model, Experimental Validation and Simulations," *Chem. Eng. Sci.*, **58**, 297 (2003).

Lin, S. X., M. Zhou, A. Azzi, G. J. Xu, N. I. Wakayama, and A. Ataka, "Magnet Used for Protein Crystallization: Novel Attempts to Improve the Crystal Quality," *Biochem. Biophys. Res. Comm.*, **275**, 274 (2000).

Qi, J. W., and N. I. Wakayama, "Suppression of Natural Convection in Non-Conducting and Low-Conducting Fluids by the Application of a Static Magnetic Field," *Material Trans., JIM*, **41**, 970 (2000).

Qi, J. W., N. I. Wakayama, and M. Ataka, "Magnetic Suppression of Convection in Protein Crystal Growth Processes," *J. of Crystal Growth*, **232**, 132 (2001).

Ramachandran, R., and F. W. Leslie, "Magnetic Susceptibility Effects and Lorentz Force Damping in Diamagnetic Fluids," AIAA-2001-0618 (2001).

Wakayama, N. I., C. Zhong, T. Kiyoshi, K. Itoh, and H. Wada, "Control of Vertical Acceleration (Effective Gravity) between Normal and Microgravity," *AIChE J.*, **47**, 2640 (2001).

Wakayama, N. I., M. Ataka, and H. Abe, "Effects of a Magnetic Field Gradient on the Crystallization of Hen Lysozyme," *J. Cryst. Growth*, **178**, 653 (1997).

Wakayama, N. I., "Magnetic Buoyancy Force Acting on Bubbles in Nonconducting and Diamagnetic Fluids under Microgravity," *J. Appl. Phys.*, **81**, 2980 (1997).

Wang, L. B., and N. I. Wakayama, "Control of Natural Convection in Non- and Low-Conducting Diamagnetic Fluids in a Cubical Enclosure using Inhomogeneous Magnetic Fields with Different Directions," *Chem. Eng. Sci.*, **57**, 1867 (2002).

Whitaker, S., "The Transport Equations for Multi-Phase Systems," *Chem. Eng. Sci.*, **28**, 139 (1973).

Manuscript received Sept. 27, 2002, and revision received Dec. 9, 2002.